

# Not eXactly Byzantine: Efficient and Resilient TEE-Based State Machine Replication

Marc Leinweber  
marc.leinweber@kit.edu  
KASTEL Security Research Labs  
Karlsruhe Institute of Technology  
Karlsruhe, Germany

Hannes Hartenstein  
hannes.hartenstein@kit.edu  
KASTEL Security Research Labs  
Karlsruhe Institute of Technology  
Karlsruhe, Germany

## Abstract

We propose, implement, and evaluate NxBFT, a practical State Machine Replication protocol that tolerates minority corruptions by using Trusted Execution Environments (TEEs). NxBFT focuses on a “Not eXactly Byzantine” operating model as a middle ground between crash and Byzantine fault tolerance. NxBFT is designed as an asynchronous protocol except for liveness of setup and recovery. As a leaderless protocol based on TEE-Rider, it provides build-in load balancing in the number of replicas, which is in contrast to leader-based and leader-rotating approaches. With quadratic communication complexity, a TEE-based common coin as source of randomness, a crash recovery procedure, solutions for request deduplication, and progress in low-load scenarios, NxBFT achieves a throughput of 400 kOp/s at an average end-to-end-latency of 1 s for 40 replicas and shows competitive performance under faults. We provide a comparison with a leader-based (MinBFT) and a leader-rotating protocol (Damysus) and analyze benefits and challenges that result from the combination of asynchrony and TEEs.

**CCS Concepts:** • Computer systems organization → Reliability; Availability; • Theory of computation → Distributed algorithms.

**Keywords:** Trusted execution, Asynchrony, Recovery

## 1 Introduction

With a known set of operators, State Machine Replication (SMR) [44] is a suitable way to operate a common service in a decentralized manner instead of commissioning the service to a single third party. The motivations for decentralized operation range from economic and organizational reasons like equitable participation to technological requirements like increased resilience, i.e., availability under high load, (network) faults, and attacks. At the core of SMR is an ordering service that orders each incoming client request before issuing the request to the business logic to keep the replicas consistent. The ordering service employs a consensus primitive (atomic broadcast) and primarily defines the level of fault tolerance and, strongly associated, the performance of the overall system.

Consensus research has been shaped by PBFT [14] and the partially synchronous timing model [26] for more than 20

years. PBFT uses a static leader that is only replaced in the event of a fault. HotStuff [53] broke with this paradigm and replaced the leader regularly (rotating leader). This paradigm shift, especially when considering streamlined [15] versions of the rotating leader family, significantly improved latency and throughput, and avoided expensive but infrequent leader changes. At the same time, asynchronous algorithms [21, 41] were also explored. These asynchronous algorithms cannot rely on a leader since no assumption can be made on delivery and processing times apart from eventual delivery. Although asynchronous methods show fundamental challenges with garbage collection, graph-based methods [21] demonstrate resilience and impressive performance.

For (partially) synchronous systems, it is well-known that Trusted Execution Environments (TEEs), e.g., in the form of small signature services that maintain an increment-only counter [19, 36], can be used to implement Byzantine fault-tolerant State Machine Replication (SMR) with an honest majority (e.g., [5, 49, 51] for static leaders and [22, 24] for rotating leaders). The motivation of TEE-based protocols is increased resilience as well as a significant gain in efficiency due to reduced communication and computation. TEE-based protocols rely on a TEE to only fail by crashing and to prevent equivocation [6, 17, 38] which requires significant trust in the TEE. TEE-Rider [34] showed how a TEE-based signature service can be used to transform DAG-Rider [33], a graph-based asynchronous atomic broadcast protocol, to withstand Byzantine faults with an honest majority.

Looking at recent incidents [10, 11], the required trust in a TEE may not be justified in arbitrary environments. However, in certain scenarios, one can build on stronger assumptions. An example we are currently working on are public transport federations [35] with tens of federation members that collaboratively operate a ticketing service based on state machine replication. For such a federation, the operators of replicas still would like to be Byzantine-tolerant, but can build on stronger trust assumptions among federation member. We therefore propose the “Not eXactly Byzantine” (NxB) operating model in which we assume that operators (1) do not attack their TEE themselves, (2) do not manipulate the business logic of their application, and (3) enable significant long phases of synchrony for “maintenance work”.

The main contribution of this paper is to show that the combination of the NxB model and the leaderless nature of graph-based protocols as given by TEE-Rider provide improved scaling performance compared to leader-based or leader-rotating approaches:

**Performance-engineered design and implementation.** Based on TEE-Rider, we designed and implemented a complete NxB fault-tolerant SMR protocol, called NxBFT. We did performance engineering by implementing a TEE-based method for quadratic communication overhead, a TEE-based common coin with no overhead after setup, and reactive recovery of crashed TEE-based replicas.

**Fundamental challenges and workaround of combination of TEEs and asynchrony.** However, while working on such a complete solution for a TEE-based and asynchronous SMR protocol, we also observed that the intricacies of the combination of TEEs and asynchrony are not yet fully explored: in particular, we show that recovery of failed replicas is more challenging with TEEs than without them. As a second contribution, we also discuss these fundamental challenges and corresponding workarounds.

**Empirical comparison of paradigms.** To evaluate scaling capabilities and performance under faults, we conducted a comparison to MinBFT [49] (static leader) and Chained-Damysus [22] (streamlined rotating leader). NxBFT achieves a throughput of 400 kOp/s at an average end-to-end-latency of 1 s for 40 replicas and shows competitive performance under faults. The results show that when the NxB fault model can be assumed, the proposed NxBFT approach can take advantage of it. Compared to MinBFT or Damysus, throughput scales through inherent load balancing with a reasonable latency penalty. Please note that our empirical evaluation is neither a benchmarking study producing absolute performance numbers nor a comparison of TEE and non-TEE-based approaches in general. The study shows the performance improvements gained by stronger assumptions (compared to Byzantine fault tolerance) and a protocol that can take advantage of these.

The remainder of this paper is structured as follows. We give an overview on related work on hybrid fault models, common coin, and recovery procedures, and also briefly introduce asynchronous and DAG-based consensus approaches in Section 2. In Section 3, we specify the assumed NxB operating model. We present an overview on NxBFT and its main building blocks in Section 4, and describe the NxBFT protocol in Section 5 in detail. Our experimental setup and empirical findings are presented in Section 6. We discuss the implications of our approach and report on our experiences in Section 7 and conclude with Section 8.

## 2 Background and Related Work

We assume the reader is familiar with the concepts of State Machine Replication (SMR) [44] and of classical Byzantine fault tolerant SMR approaches like PBFT [14].

### 2.1 Hybrid Fault Models

Hybrid fault models have been investigated for at least two decades [18]. Their core idea is to equip replicas with a trustworthy subsystem that is assumed to only fail by crashing. Replicas have to use the trusted subsystem to produce valid messages. The trusted subsystem enforces non-equivocation: a replica cannot send two messages with different contents to different peers in the same context without being noticed [16, 17, 19, 38]. The non-equivocation property saves rounds of communication and allows operating Byzantine fault tolerant (BFT) SMR with an honest majority ( $n > 2f$ ) [16–18, 49]. With the advent of hardware-based Trusted Execution Environments (TEEs) like Intel SGX [20], researchers were able to propose the first practical systems using a trusted subsystem in the partially synchronous models adopting ideas from PBFT [5, 36, 37, 49]. These works rely on a TEE to provide confidential execution of code. Additionally, a TEE must also be able to remotely attest to the integrity of itself and code running on it. The TEE implements a signature service that maintains an increment-only counter. If a replica wants to broadcast a message, it has to attach a signature and a corresponding counter produced by its TEE. Receiving replicas will only accept one message for each possible counter value for each replica. Under the assumption that the TEE will assign each counter value only once, receiving replicas can be sure that they all see the same message for the same counter value. Recent work focuses on the rotating leader paradigm [22, 24], the asynchronous [28, 34] timing model, and alternative trusted subsystems [2]. We build upon the findings for the asynchronous timing model using Intel SGX to derive our TEE model. We show, in contrast to Gupta et al.’s claim [30], that trusted subsystems allow a highly parallelized and efficient consensus protocol design (as also stated by Bessani et al. [8]).

### 2.2 DAG-Based Total Order Broadcast

Until the publication of HoneyBadgerBFT [41], asynchronous protocols were considered inefficient and more of theoretical interest. Recent advances, however, have shown that asynchronous consensus protocols promise increased resilience and throughput while at the same time being less complex than their partially synchronous counterparts [21, 41]. Hashgraph [4] and DAG-Rider [33] were among the first asynchronous consensus protocols building upon a directed acyclic graph (DAG) that encodes the logical chronology of messages exchanged, comparable to a causal order broadcast. In a second step, the total order of transactions is derived using a deterministic graph traversal. In contrast

to Hashgraph (and its TEE variant [28]), DAG-Rider simplifies the consensus derivation and the message exchange by building the graph deterministically. Narwhal [21] improves on DAG-Rider, especially the messages exchanged were reduced from  $O(n^3)$  to  $O(n^2)$ . TEE-Rider [34] showed that DAG-Rider can be compiled to withstand Byzantine faults with  $n > 2f$  replicas using a signature service as described in the previous subsection. Yandamuri et al. [52] showed how to reach quadratic communication complexity in the worst case using a small TEE in an asynchronous environment. NxBFT builds upon TEE-Rider (cf. Section 4) to facilitate scaling throughput and for its less complex implementation; it further improves ideas from Narwhal to reach quadratic communication complexity as well. Bullshark [48] optimizes Narwhal for partial synchrony and introduces a time-based garbage collection. Recently, Shoal [47] proposed pipelining and a reputation-based leader election for the DAG-Rider protocol family. The investigation of the compatibility of Shoal with NxBFT is left for future work. BBChain [40], Sailfish [45], Shoal++ [3], and Autobahn [29] optimize the end-to-end latency of DAG-based protocols for partially synchronous systems. Bandle [50] investigates asynchronous protocols for crash fault environments adopting similar concepts as NxBFT for common coin and low-load scenarios. We refer to Section 7 for a discussion.

### 2.3 Common Coin

Asynchronous consensus protocols rely on randomness to circumvent the FLP impossibility [7, 27]. TEE-Rider uses a uniformly distributed common coin [13, 43] that produces a value from the interval  $[0, n - 1] \subset \mathbb{N}_0$ . Each coin toss has a unique “name”, in case of TEE-Rider the wave number, and a coin toss will be successful as soon as a pre-defined threshold of replicas, e.g.  $f + 1$ , requests it. This property ensures that attackers cannot learn a random value before at least one correct replica tries to learn it. Typically, common coins are implemented using threshold signatures (e.g., [9]). Abraham et al. [1] suggest a common coin based on dealer-based verifiable secret sharing for their asynchronous TEE-based binary consensus protocol. We argue that, when already using a TEE, it seems rational to avoid the use of rather expensive cryptographic computations. Jia et al. [32] propose a synchronous TEE-based common coin incompatible with TEE-Rider. We propose a TEE-based common coin that uses the received vertices to verify that a coin toss is allowed, incurring no overhead after a dealerless setup.

### 2.4 Crash Recovery and Reconfiguration

When replicas experience unintended faults, e.g., in the case of hardware failures or simply when doing maintenance or updates, they miss state updates and cannot participate anymore. A recovery procedure allows a replica to catch up and be able to produce valid messages and decide on the validness of received messages [25]. PBFT [14] implements a

checkpointing mechanism usable for recovery. A TEE-aware recovery procedure requires the establishment of a new signature secret and it has to bring all correct replicas “on the same page” concerning the messages broadcast by the recovering replica. A recovery mechanism can be extended to support reconfiguration: replicas may join or leave the peer-to-peer network based on the ongoing consensus algorithm. To the best of our knowledge, CCF [31] is the only TEE-based SMR system offering reconfiguration. CCF, based on ENGRAFT [51], operates in partial synchrony and uses specifically crafted client requests for recovery. We show that such an approach is incompatible with the asynchronous nature of NxBFT’s atomic broadcast.

## 3 Not eXactly Byzantine: Operating Model

We consider a federated peer-to-peer system with  $n$  predefined operators. The federation operates and offers a common service using State Machine Replication (SMR) for an arbitrary number of clients. Each operator operates a replica;  $f < \frac{n}{2}$  replicas may behave Byzantine. We assume replicas to execute the same non-manipulated state machine limiting operators to omission faults when communicating with clients. Each replica is equipped with a Trusted Execution Environment (TEE) capable of running arbitrary code (called enclave) that offers confidential and integrity protected computing as well as remote attestation to verify the authenticity of the TEE and its enclave. The TEE can confidentially and authentically export (partial) enclave state (“sealing”). The TEE is assumed to only fail by crashing; its internal state is lost when crashing. If not explicitly stated, code is not executed inside the TEE. Replicas and clients communicate via secure point-to-point links. Messages can be reordered and arbitrarily delayed but not dropped. Setup and recovery require synchrony for liveness. Clients may be Byzantine faulty.

## 4 NxBFT: Overview

NxBFT builds upon TEE-Rider [34], a leaderless, TEE-based and asynchronous atomic broadcast protocol that maintains a grow-only directed acyclic graph (DAG) that is structured in rounds. Each replica is equipped with a TEE that offers a signature service and a common coin. With the exception of setup and recovery, NxBFT operates asynchronously. NxBFT is structured in three layers (see Figure 1): application, consensus, and broadcast. In the following, we describe a full Request–Broadcast–Consensus–Response cycle.

**Request.** Clients are the users of the federated service. The NxBFT-relevant client state consists of a client id, a sequence number, and the identities of the replicas. When a client wants to use the service, it composes a request containing the command and the current value of the sequence

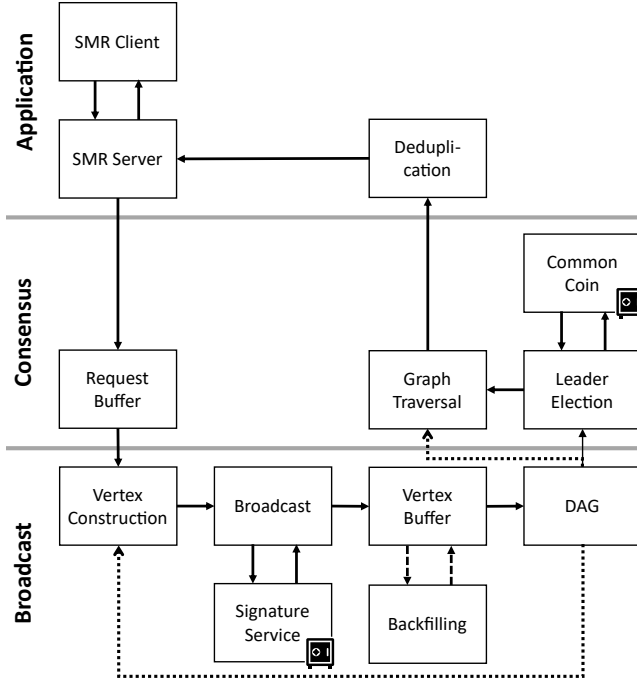


**Figure 1.** NxBFT components. The safe icon marks components executed in the TEE. Solid arrows show the flow for a client request to be successfully ordered and executed. After being received by the replica, a request is buffered and eventually broadcast as a vertex payload using TEE-based signatures. A vertex is added to the DAG when its ancestry was already added (optional backfilling, dashed arrows). Each added vertex will eventually be ordered by a graph traversal; the corresponding root is selected using a common coin. After request deduplication, the request is output to the application layer and the response sent to the client. The dotted arrows highlight components using the DAG as input.

number variable and sends the request to a replicas. Receiving replicas will buffer the request until it can be included in the payload of a broadcast round.

**Broadcast.** In each round  $r$  of the broadcast layer, each replica has to propose a new DAG vertex containing client requests to be ordered. Vertices  $v$  are bound to a round  $v.r$  and broadcast in a best effort fashion. NxBFT uses a TEE-based signature service as described above to prevent equivocation on the broadcast layer. The counter of the signature service is used to enforce a FIFO ordering, i.e., a message with lower counter value must be delivered before a message with higher counter value can be delivered. If received vertices contain an already processed counter value, they are dropped. Thus, faulty replicas are limited to omission faults. A vertex needs to reference  $\lfloor \frac{n}{2} \rfloor + 1$  vertices of the previous round as edges and needs to be signed by the corresponding TEE-based signature service. Correct replicas will always reference their own vertex of the previous round as an edge.

Due to asynchrony, vertices for rounds  $v.r < r$  or  $v.r > r$  can be received any time. Thus, received valid vertices are buffered until they can be added to a replica’s local DAG. A vertex can be moved from buffer to DAG if the replica already transitioned to the vertex’ round and the replica’s DAG contains all referenced vertices of a new vertex. By transitively applying this requirement, the *complete* ancestry of a newly added vertex must already be part of the DAG. If vertices of the ancestry are missing, the replica will ask its peers to retransmit said vertices (backfilling). Signature service and backfilling “upgrade” the best effort broadcast to a reliable broadcast. DAG construction and reliable broadcast combined build a causal order broadcast [12, Module 3.9]; the DAG encodes the causal order of exchanged messages. A replica completes round  $r$  and transitions to the next broadcast round  $r + 1$  when it added at least  $\lfloor \frac{n}{2} \rfloor + 1$  valid vertices for round  $r$  to the DAG.

**Consensus.** Every (disjoint) four consecutive completed broadcast rounds are grouped into a *wave*: round  $r$  belongs to wave  $w = \lceil \frac{r}{4} \rceil$ . When a wave  $w$  is completed, that is, its fourth round is completed, the consensus layer is invoked: It tries to derive agreement on a total order of requests of wave numbers smaller than  $w$  for all correct replicas. Essentially, the wave construction works as follows. Assume a wave  $w$  is complete. A vertex of the first round of wave  $w$  is selected as wave leader; since the TEE-based common coin is used for selection, all correct nodes select the same vertex. The wave number  $w$  is used as the name for the coin toss. If the wave leader is part of a replica’s local DAG when it is selected and at least  $\lfloor \frac{n}{2} \rfloor + 1$  vertices of  $w$ ’s fourth round have a path to it (“direct commit rule”), the replica can commit the wave: The wave leader is then used as starting point for a pre-defined deterministic graph traversal to order all not yet ordered requests of previous waves. If the wave leader is not part of the DAG, the wave cannot be committed yet. A replica will check during direct commits of future waves if it can retrospectively commit a wave. For a retrospective commit, a single path between old and new wave leader is sufficient. The construction of a wave ensures a “common core” that guarantees that the leader of the next wave (and all future waves) has a path to the previous leader. For proofs of correctness, we refer the reader to [34, Lemma 3] and [33, Proposition 2]. However, it is important to note that the consensus layer works solely on the local DAG without any additional communication. A correct replica will be able to commit every second wave in expectation.

**Response.** The requests are executed by the server-side application in the order they were added to the vertex by the proposing replica. The sequence number of a request is used for deduplication: the combination of client id and sequence number is output exactly once to the application. After execution, the result is sent as a response to the initially requesting client.

## 5 Nx-BFT: Protocol

### 5.1 Throughput Scaling

**Client and Request Handling.** A client selects a replica at random and unicasts its request accompanied with a client id and a sequence number. Once the consensus layer decided, all correct replicas will input the request to the state machine. The output of the state machine is then sent to the client as a response. Following the Nx-B operating model (Section 3), replicas will only commit omission faults when communicating with clients, and, thus, this single response is sufficient for the client to complete the request. Once the request is completed, the client increments its sequence number by one. This client and request handling mechanism allows each replica to propose a disjoint set of requests in each round scaling up throughput with the number of replicas.

The client cannot be sure that the selected replica will answer, e.g., due to omission to the client or faults of the replica on the consensus layer. When the client issues its request, it starts a timer. If the selected replica does not answer within the time interval, the client selects a different replica for its request, starting a new timer. Due to the properties of the consensus layer, the client is now guaranteed that its request will be ordered, however, a request can appear in the DAG up to  $n$  times, and be output to the application up to  $n$  times. Therefore, to reduce the load for the application, Nx-BFT employs a simple deduplication logic: a correct client will only have one unanswered request at a time. The replicas store for each client the client’s last ordered sequence number. Whenever a request is encountered during the graph traversal determining the order, the request is only input to the state machine when its sequence number is greater than the stored sequence number. If a client issues more than one request simultaneously, i.e., behaves Byzantine, it is possible that some of its requests will not be answered due to the deduplication mechanism.

**Low-Load Scenarios.** Asynchronous algorithms typically rely on valid messages from peers to make progress (see, e.g., [33, Algorithm 2]). In the case of TEE-Rider, a replica needs at least  $\lfloor \frac{n}{2} \rfloor + 1$  valid vertices for its current round to transition to the next round and to be allowed to broadcast its next vertex. To increase the achievable throughput, a replica would hold back its vertex until it can propose at least a certain amount of client request as the vertex’ payload. If now only a few clients issue requests, the system would come to a halt as the quorum for a round to complete would need a lot of time to be established. However, this problem is not introduced by Nx-BFT’s client behavior but worsened. TEE-Rider and Narwhal suffer from a similar issue. We address this issue by working with (local) timers on the side of the replica. A replica will start a timer when it transitions to a new round. When the replica is able to broadcast a vertex containing enough client request within the time interval, it will cancel the timeout. On timeout, however, the replica

is allowed to broadcast an empty vertex. This allows other replicas to complete the round.

**Backfilling-Based Reliable Broadcast.** Instead of a proactive TEE-based single echo reliable broadcast (e.g., [19, Algorithm 1]) with  $O(n^2)$  messages exchanged as used by TEE-Rider (cf. Figure 2a), we use a backfilling strategy, thus, correct replicas do not echo vertices. Instead, if an ancestor is unknown, i.e., it was neither already added to the DAG nor buffered, a request for the missing vertex is sent to all replicas. Due to asynchrony, correct replicas cache vertex requests if they cannot answer them directly: It is possible that the corresponding vertex arrives delayed and the replica receiving the vertex request is the only correct replica that receives the requested vertex due to faults by the sender. A different option would be for replicas to repeat their request after some time trading potentially unbounded memory consumption with algorithmic complexity.

Since we use the signature service to implement a FIFO broadcast with non-equivocation, we get ‘no duplication’, ‘integrity’, and ‘consistency’ as reliable broadcast properties [12, Module 3.12] for free. The backfilling mechanism is solely responsible for validity and totality: If a correct replica broadcasts or delivers a message, every other correct replica will deliver this message. Correct replicas will only use vertices as edges that they already added to their DAG. This behavior implies that those edges are valid vertices with a completely known ancestry. If a replica now receives a vertex for which it does not know an edge, this is due to two reasons: (1) the edge is from a correct replica and the corresponding vertex was not yet delivered by the asynchronous channel or (2) the edge is from a faulty replica that committed a send omission fault. In case (1), our replica will receive the edge eventually and validity and totality will be preserved. In case (2), if at least one correct replica received the vertex and was able to add it to the DAG, no matter if itself used the vertex as an edge or not, the replica will be able to answer any vertex request, thus, fulfilling totality. If no correct replica received the vertex, no correct replica will deliver the vertex, thus, not breaking totality.

In TEE-Rider, a replica echos each vertex once leading to  $n^2 + n^3$  messages per broadcast round (Figure 2a). Narwhal uses a three-way handshake to produce quorum certificates that certify the availability of vertices. Those quorum certificates have to be attached to the next vertex to be valid. In contrast to Narwhal, we can save a constant communication factor as we do not rely on quorum certificates. In the common case, Narwhal needs  $3n^2$  messages per broadcast round (Figure 2b), whereas Nx-BFT proceeds with one  $n^2$  communication step (Figure 2c). In the worst case, both send up to  $n$  backfilling requests to all replicas and receive  $n$  replies, leading to  $5n^2$  messages for Narwhal vs.  $3n^2$  messages for Nx-BFT per broadcast round.

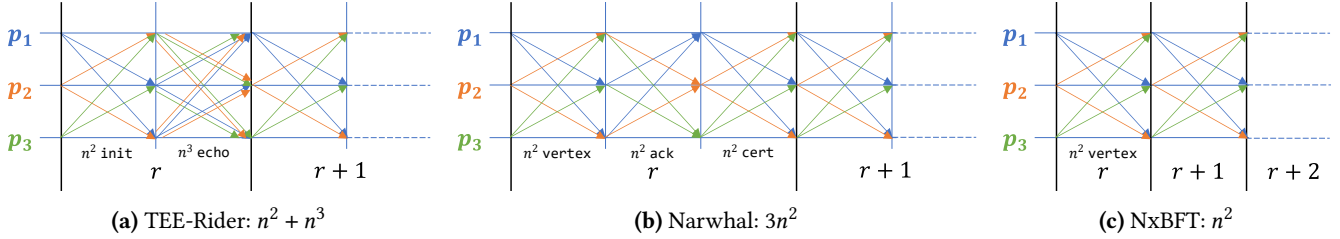


**Figure 2.** Common case communication patterns of TEE-Rider [34], Narwhal [21] and NxBFT (this work). Blue vertical lines delimit communication rounds, black vertical lines delimit rounds of the broadcast layer. The colors of the arrows signify the payloads’ originator. NxBFT proceeds with one round of communication per broadcast round.

## 5.2 Enclave

The enclave of NxBFT, its trusted subsystem, has two tasks. It implements a signature service with an increment-only counter akin to MinBFT [49] or TrInc [36] and it offers a common coin. The common coin is based on a cryptographically secure pseudorandom number generator (PRNG) that is initialized with a common seed during setup. To be able to toss a coin, a replica has to convince the coin implementation that it made sufficient progress on the consensus layer, i.e., it completed enough rounds. In the following, we will explain the inner workings in more detail; the pseudocode can be found in Algorithm 1. We use the term *(public/secret) enclave keys* to refer to the keys used for the signature service in contrast to the *(public/secret) replica keys* used for authenticated communication between replicas. Enclave keys are volatile in the sense that they must be lost when a replica crashes. Their safe replacement is the focus of the recovery protocol (see Section 5.3).

**Signature Service.** The signature service is used to enforce non-equivocation on messages. Each signature is accompanied with a unique counter value. Receiving replicas accept only one message per counter value. On initialization, each enclave generates an asymmetric key pair used exclusively for the signature service and sets its counter value  $c$  to 0. Attestation certificates generated by an enclave contain its public enclave key and are signed with a replica key during setup and recovery in order to establish a binding between these two key pairs. The attestation additionally binds enclave keys to the current execution environment and ensures that they correspond to actual peering enclaves. Thus, enclaves learn the public enclave keys of each other when verifying attestations. When a replica now requests a signature for a message by calling  $sign()$ , the enclave signs the combination of message and current counter value with its secret enclave key, increments its counter by one, and returns signature and corresponding counter. When asked for verification with  $verify()$ , the enclave combines counter and message and checks the signature to match using the corresponding public enclave key that it accepted during setup or recovery. The above verification and attestation are

not required to be executed inside the TEE; we do this to ease the implementation of the common coin.

**Common Coin.** NxBFT uses the common coin to select a wave leader for each wave, i.e., it tosses a number in the interval  $[0, n - 1] \subset \mathbb{N}_0$ . For NxBFT to maintain its safety guarantees, the common coin needs to be fair, it must produce the same output for every replica and wave, it must not be predictable until at least  $\lfloor \frac{n}{2} \rfloor + 1$  replicas tossed for a wave, and it has to be revealed when at least  $\lfloor \frac{n}{2} \rfloor + 1$  replicas toss for a wave.

On initialization, each enclave generates a random bit string used as a *seed share* that is encrypted during setup and sent to peering enclaves. The enclave combines all  $n$  received seed shares using the XOR operation to derive the common seed. We use the resulting random bit string to seed a PRNG. The coin implementation allows a coin toss whenever it can be convinced that four rounds of NxBFT’s broadcast layer were successfully completed by the replica. The implementation maintains a variable  $rToss$  that is initially set to four and resembles the expected round in which a coin toss is allowed. When a replica wants to learn the next coin value by calling  $toss()$ , it has to provide at least  $\lfloor \frac{n}{2} \rfloor + 1$  validly signed vertices of different replicas and the expected round ( $v.r = rToss$ ), proving the round was completed by at least one correct replica. The vertex struct carries the vertex creator, the enclave signature  $\sigma$ , and the enclave counter  $c$  as payload to allow signature verification. If the replica supplied sound evidence, the implementation will increment  $rToss$  by four, i.e., to point at the next wave’s end, and return the next value of the PRNG.

The XOR construction is a variant of the straightforward  $t = n$  secret sharing; the resulting seed is kept confidential by the secure communication and the TEE. The enclave will not reveal a toss unless at least one correct replica requests a toss. A correct replica will always toss a coin when it completes the last round of a wave and proposed its own vertex for it, enabling every correct replica to learn the coin value as soon as possible. Note that it is not necessary to use the TEE-based signatures, as we do, to achieve the desired properties, but it makes implementation easier.

**Algorithm 1** Nx-BFT Enclave: Setup and Operation

---

```

1: state  $(sk, pk)$ : asymmetric key pair
2: state  $n, c, rToss, peersAdded$ :  $\mathbb{N}_0$ 
3: state  $replicaKeys, enclaveKeys$ : array of public key
4: state  $seed, seedShare$ : 256 bit string
5: state  $rng$ : cryptographic PRNG
6: state  $ready$ : boolean
7: function  $init(peerList)$ 
8:   if  $ready$  then return
9:    $replicaKeys \leftarrow peerList; enclaveKeys \leftarrow [\perp, \dots, \perp]$ 
10:   $n \leftarrow |peerList|; replicaKeysAdded \leftarrow 0; c \leftarrow 0$ 
11:   $rToss \leftarrow 4; ready \leftarrow \text{False}$ 
12:   $seed \leftarrow 0 \dots 0$ 
13:   $(pk, sk) \leftarrow \text{generate asymmetric key pair}$ 
14:   $seedShare \leftarrow \text{generate random 256 bit string}$ 
15: function  $getAttestationCertificate()$ : attestation
16:   return  $createAttestation(pk)$   $\triangleright$  TEE function
17: function  $attestPeer(p_k, att, \sigma)$ : bit string
18:   if  $ready \vee \neg \text{attest}(att) \vee \neg \text{vfy}(\sigma, replicaKeys[p_k], att)$ 
   then return  $\perp$ 
19:    $enclaveKeys[p_k] \leftarrow att.p_k$ 
20:   return  $encrypt(enclaveKeys[p_k], seedShare)$ 
21: function  $addPeer(p_k, ciphertext)$ : boolean
22:   if  $enclaveKeys[p_k] = \perp \vee ready[p_k]$  then
23:     return  $\text{False}$ 
24:    $share \leftarrow \text{decrypt}(sk, ciphertext)$ 
25:   if  $share$  is error then return  $\text{False}$ 
26:    $seed \leftarrow seed \oplus share$ 
27:    $peersAdded \leftarrow peersAdded + 1$ 
28:    $ready[p_k] \leftarrow \text{True}$ 
29:   if  $peersAdded = n$  then
30:      $rng.init(seed); ready \leftarrow \text{True}$ 
31:   return  $\text{True}$ 
32: function  $sign(m)$ :  $(\mathbb{N}_0, \text{signature})$ 
33:    $\sigma \leftarrow \text{sgn}(sk, (c, m)); c \leftarrow c + 1; \text{return } (c - 1, \sigma)$ 
34: function  $verify(p_k, m, c, \sigma)$ : boolean
35:   return  $\text{vfy}(\sigma, enclaveKeys[p_k], (c, m))$ 
36: function  $toss(vs)$ :  $\mathbb{N}_0$ 
37:   if  $\neg ready$  then return  $\perp$ 
38:    $valid \leftarrow 0; seen \leftarrow \text{empty set}$ 
39:   for  $v \in vs$  do
40:     if  $seen.contains(v.creator)$  then continue
41:     if  $v.r = rToss \wedge \text{verify}(v.creator, v, v.c, v.\sigma)$  then
42:        $valid \leftarrow valid + 1; seen.insert(v.creator)$ 
43:   if  $valid < \lfloor \frac{n}{2} \rfloor + 1$  then return  $\perp$ 
44:    $rToss \leftarrow rToss + 4$ 
45:   return  $rng.uniform(0, n)$ 

```

---

**Setup.** During setup, Nx-BFT enclaves mutually attest and verify their integrity, reach consensus on the deployed enclave code as well as the peers' public enclave keys to prevent simulation attacks, and establish the authenticated channels between replicas. The second objective of the setup protocol is to initialize the PRNG underlying the common coin with a collaboratively generated random seed. Due to the required participation of all  $n$  replicas in both of the above tasks, Nx-BFT cannot tolerate but reliably detect faults during setup. We construct the setup protocol using  $n$  synchronous authenticated reliable broadcast instances with a fault tolerance of  $n > f$  [42] to preempt equivocation by faulty replicas. In the following, we describe the setup protocol of Nx-BFT as a one-way handshake between replicas  $p_i$  and  $p_j$ , at the end of which  $p_j$  will have attested  $p_i$ . A replica  $p_i$  also performs this setup handshake with itself. A replica has completed its setup once it has completed all of its  $n$  handshakes and attested all replicas.

A replica  $p_i$  is initialized with its own identifier  $id \in [0, n-1] \subset \mathbb{N}_0$ , its secret replica key, and an array mapping the ids of all replicas to their public replica keys, thus establishing authenticated communication channels. By calling  $init()$  with the array of public replica keys, the replica initializes its enclave. Upon initialization, the enclave of  $p_i$  initializes its state variables and generates both a new enclave key pair and a random seed share for the later initialization of the common coin PRNG. Next,  $p_i$  obtains its own attestation certificate from its enclave ( $getAttestationCertificate()$ ), which includes the newly generated public enclave key that will be used in the signature service. To bind its current public enclave key to its public replica key,  $p_i$  signs its attestation certificate with its secret replica key.

Replica  $p_i$  now uses a synchronous authenticated single-echo reliable broadcast to disseminate its identifier and its signed attestation certificate using *Hello* and *HelloEcho* messages. Replica  $p_j$  receives a Hello message directly from  $p_i$  and  $n$  HelloEcho messages from all replicas. If the contents of all messages originating from  $p_i$  agree with each other, the signature of the attestation certificate verifies against  $p_i$ 's public replica key, and  $p_j$ 's enclave accepts  $p_i$ 's attestation certificate as valid, then  $p_j$ 's enclave accepts  $p_i$ 's enclave key and produces an encryption of its seed share using said enclave key in the function  $attestPeer()$ . Replica  $p_j$  then sends this encrypted seed share to  $p_i$  in a *HelloReply* message, thereby completing its part of the handshake. Since the enclave of  $p_i$  needs to accept  $p_j$ 's enclave key before it can process the payload of the HelloReply message, such messages are buffered until then. Replica  $p_i$  then calls the enclave function  $addPeer()$  with the encrypted seed share, which is decrypted and XOR'd together with the current seed value. After all  $n$  seed values are combined in this way, the common coin PRNG is initialized with the resulting seed. Once a replica has completed all  $n$  handshakes, it has completed the setup protocol and broadcasts a *Ready* message



to all replicas. After the receipt of  $n$  Ready messages, the asynchronous operation of the SMR protocol can commence.

Replicas start a timer for each handshake when sending the Hello message, the expiration of which raises an error and leads to an abortion of the entire setup. Similarly, conflicts between Hello and HelloEcho messages of a particular replica or invalid signatures or attestation certificates raise errors and lead to an abort.

### 5.3 Crash Recovery

Faults like hardware failures, human configuration errors, and maintenance require that a replica can be put back into the condition to validate received messages and produce valid messages. We are interested in an algorithmic solution that can recover replicas while allowing the system to continuously operate. Such a recovery procedure must ensure that the recovery does not allow (1) equivocation and (2) to learn coin values beforehand. For NxFT in particular, the recovery procedure has to be aware of the TEE and its state. We first present two challenges one is facing in the design of a recovery procedure for NxFT. Then we present a recovery procedure that is Byzantine safe under asynchrony but requires participation of *all* replicas for liveness.

**Impossibility Conjecture.** NxFT’s only active agreement primitive is an asynchronous TEE-based reliable broadcast with a fault tolerance of  $n > f$ . From the reliable broadcast message history and state, the graph and all decisions are passively derived. Thus, recovering a NxFT replica is, for the most part, recovering the reliable broadcast module leading to two issues: (1) the recovery procedure cannot use the ongoing graph-based consensus for coordination and (2) it is impossible to use a quorum-based decision for recovery.

We explain the first impossibility with the following example. Assume three replicas Alice, Bob, and Charlie with Charlie trying to recover and broadcasting a specially crafted request containing its new public enclave key authenticated with Charlie’s “long-living” public replica key (input to all during setup). Alice and Bob both receive Charlie’s request, propose it for ordering, and eventually reach consensus. Due to asynchrony, after reaching consensus on the recovery, Alice receives a vertex from Charlie signed with the old enclave key. Consequently, she will reject it. Bob, however, received the same vertex before reaching consensus with Alice and accepted it. If both now sort their graphs, they will get different orderings breaking the consensus layer’s safety. Even when requesting the vertex from Bob because he references it in his vertex, Alice has no possibility to judge on Bob’s and Charlie’s honesty. Thus, if multiple identities of a peer’s enclave exist simultaneously, equivocation can happen.

Recovery requires all correct replicas to reach agreement on the valid vertices of the recovering replica. Additionally, the input of all correct replicas to such a decision has to be

honored. This forbids a quorum-based approach, as any quorum reached in asynchrony may outvote a correct replica: In a TEE-based reliable broadcast with a fault tolerance of  $n > f$ , a receiving replica can, on successful signature verification, deliver immediately. Therefore, a correct replica Alice at an arbitrary but fixed point in time may be the only correct replica having delivered a certain value, e.g., of Bob. This is not in conflict with the totality property as Alice will relay the value and eventually all correct replicas will deliver as well. If Bob now crashes and recovers, all correct replicas need to agree on what Bob sent and what was potentially delivered. Any quorum smaller than  $n$ , no matter if  $n > 2f$  or  $n > 3f$ , has a chance to outvote Alice: due to asynchrony, there is neither a guarantee that all votes building the quorum are cast by correct replicas nor that the votes used for a quorum are the same for all correct replicas. Thus, there exist traces in which Alice would need to “undeliver” already delivered values breaking the desired properties of reliable broadcast. If now any precondition is lifted, i.e., asynchrony, prevention of rollbacks, or TEEs preventing equivocation, this impossibility does not hold anymore.

**Recovery Protocol.** The recovery protocol is a variation of classical interactive consistency [42] and Fischer et al.’s consensus without faults [27, Sec. 4]. The recovery protocol assumes correct operators to create a backup of state and enclave at least after setup and every successful recovery. The enclave backup uses sealing and contains all state except the secret enclave key and the counter value. To circumvent the introduced impossibilities, the protocol requires the input of *all* replicas to reach a recovery decision. Based on the backed-up state, a recovering replica requests a recovery consensus of all replicas by broadcasting a *RecoveryRequest* message. Replicas that receive the request will initialize a consensus procedure to achieve agreement on the recovering replicas message history among all  $n$  replicas.

We assume that  $r \leq f < \lfloor \frac{n}{2} \rfloor + 1$  replicas request to recover<sup>1</sup>; a recovering replica must not fail during recovery. First, the recovering replica  $p_k$  will try to recover the enclave by providing an encrypted enclave state export. The replica  $p_k$  broadcasts a *RecoveryRequest* with the new attestation certificate including  $p_k$ ’s new public enclave key. A receiving replica  $p_i$  will verify the attestation, delete all buffered vertices that belong to  $p_k$ , and identify all vertices of  $p_k$  in its graph, i.e.,  $p_k$ ’s message history. Finally,  $p_i$  broadcasts a *RecoveryProposal* for  $p_k$  with  $p_k$ ’s new attestation certificate and the message history as payload. RecoveryProposals are reliably broadcast using relaying by receiving replicas and can be accepted once all, i.e.,  $n - r$ , relays are received and match (synchronous authenticated single-echo reliable broadcast). As soon as  $n - r$  RecoveryProposals with equal

<sup>1</sup>If a correct replica fails while the recovery protocol is running for  $r$  replicas, the recovery protocol will restart and recover  $r + 1 \leq f$  replicas as soon as the now failed replica requests its recovery.



attestation certificates are accepted, a correct replica  $p_i$  will identify the proposal with the longest valid vertex chain and broadcast it along with  $p_k$ 's new attestation certificate as a *RecoveryCommit*. Each replica signs a *RecoveryCommit* with their secret replica key. On the receipt of  $\lfloor \frac{n}{2} \rfloor + 1$  consistent *RecoveryCommits*, a replica  $p_i$  is able to complete the recovery procedure. Replica  $p_i$  will add all unknown vertices from the commit to the vertex buffer and set the expected counter value for  $p_k$  to 0. Additionally,  $p_i$  will provide the new attestation certificate of  $p_k$  and the signatures from the collected *RecoveryCommits* to its enclave. On success verification, the enclave will exchange the public enclave key for peer  $p_k$ ;  $p_i$  can now process new messages of  $p_k$ . The recovering replica  $p_k$  will derive the first round it is allowed to propose a new vertex for from the *RecoveryCommits*; missed vertices are fetched using the backfilling mechanism.

**Correctness.** Obviously, the proposed protocol is only live if all replicas are eventually reactive. Byzantine faulty replicas can stop the recovery procedure by not sending a *RecoveryProposal* at any time (or an invalid one). In the following, we will argue on the Byzantine safety of the recovery protocol and the liveness for the recovering replica if all replicas participate. To prevent that the recovery protocol enables equivocation, the enclaves of all correct replicas must replace the recovering replica's enclave key with the same key (i.e., agreement on the attestation certificate). The signature verification in the enclave enforces that the replica collected  $\lfloor \frac{n}{2} \rfloor + 1 > r$  *RecoveryCommits*. Thus, at least one correct replica collected all  $n - r$  *RecoveryProposals* that contained the same attestation certificate implying agreement. Since *RecoveryProposals* are reliably broadcast (i.e., non-equivocation for message history proposals), all correct replicas apply the exact same vertices of a recovering replica when they identify the longest valid vertex chain. The common coin is recovered by importing the enclave state, including the seed established during setup, and fast-forwarding the PRNG state to be directly "before" the next toss the replica would have made when not crashing. Thus, the coin implementation will only reveal new coins whenever the replica can prove the needed progress of the system (with or without the replica's contribution) to its enclave. As the common coin uses the public enclave keys, the agreement on the attestation certificates ensures that a Byzantine faulty replica cannot learn coin values in advance.

## 6 Practical Evaluation

We investigate the scaling behavior of NxBFT with varying payload sizes, the behavior under faults, and the impact of the NxB client in comparison to MinBFT [49, Sec. 4] and Chained-Damysus [22, Sec. 7].

### 6.1 Experiment Setup and Implementation

We use the ABCperf framework [46] written in Rust as the basis for our experiments. ABCperf orchestrates the experiment, implements the full communication stack, and handles performance measurement. Based on the application layer, ABCperf emulates the client behavior (either following the BFT or NxB rules). ABCperf ships a no-op application with random byte payloads and a MinBFT implementation; we add NxBFT and Chained-Damysus (own implementation based on [22, Sec. 7]) as atomic broadcast modules.

We run our experiments on a cluster of 25 servers of which we use 20 for replicas (Intel E-2288G, 64 GB main memory), four for client emulation (AMD EPYC 9274F, 128 GB main memory) and one as an orchestrator (Intel E-2288G, 64 GB main memory). The actual number of replicas is equally distributed among the 20 replica hosts. All servers are connected with 10 GBit interfaces.

A single experiment run has the following pattern: the replicas are setup and perform the setup phase of the atomic broadcast algorithm. Then, we start to invoke client requests following a configurable constant frequency ("request rate"). A client has at most one open request. Now, whenever a request is to be made, the client emulator checks if it has an idle client, i.e., a client with no pending request, and issues the request according to the NxB (random selection with fallback, one valid answer suffices) or BFT (broadcast,  $\lfloor \frac{n}{2} \rfloor + 1$  valid answers required) client models. To prevent crashes of emulation and experiment framework due to resource exhaustion, we have to limit the client number to 750000. After a pre-defined warm-up phase in which the request rate is increased until we reach the desired configuration, the measurement phase starts. We measure the end-to-end latency of each request as the elapsed time, observed by a client, between sending a request and getting a valid answer. The achieved throughput is the number of successfully completed requests per second.

To ease implementation and, foremost, testing, the atomic broadcast state machines do not use any form of parallelism. We deem this to be reasonable as we are not interested in actual numbers that can be expected for production deployments but the relative behavior of the three algorithms at investigation. ABCperf's communication stack and client emulation, however, are highly parallelized (on top of Tokio<sup>2</sup>). All enclave code is executed with Intel SGX [20]. Although we are aware of the limitations and weaknesses of SGX (e.g., [11]), in our experiments SGX serves as a viable way to account for the overhead of enclaved execution. To ensure a correct implementation of NxBFT, we employ a combination of unit and randomized integration tests. We use randomization for omission fault emulation and message reordering.

We report on those algorithm parameters that brought the best performance in a manual sensitivity analysis. Batching

<sup>2</sup><https://tokio.rs/>

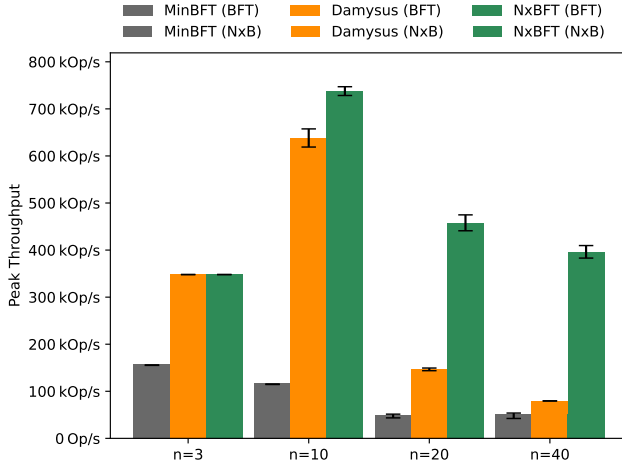


**Figure 3.** Peak throughput of MinBFT, Chained-Damysus, and NxBFT; average of eight runs. The error bars indicate the 95% confidence interval, the hatched areas the achieved throughput when using a BFT client instead NxB.

is configured as follows: MinBFT requires a block to contain at least 10000 requests, Damysus and NxBFT require 100 requests. To prevent request starvation, all algorithms propose at least every 0.1 s a new block which may be empty if a replica did not receive a request since proposing the last block. MinBFT uses an exponentially increasing timer for timeouts. Chained-Damysus uses the exponential increase and linear decrease as described in the paper [22, Sec. 3]. MinBFT and Chained-Damysus have an initial timeout value of 3 s. The fallback timeout of the NxB client is 5 s.

## 6.2 Throughput Scaling

To evaluate scaling behavior, we run NxBFT, Chained-Damysus, and MinBFT with request rates between 50 kOp/s and 800 kOp/s (step: 50 kOp/s) for  $n \in \{3, 10, 20, 40\}$  replicas. To prevent measuring network speed and implementation quality of, e.g., hashing and, instead, investigate the protocols' overhead, the requests have a zero byte payload. Each configuration is executed eight times.

Figure 3 shows the achieved peak throughputs. MinBFT achieves its peak throughput for  $n = 3$  with  $\sim 150$  kOp/s. Chained-Damysus' and NxBFT's throughput peaks at  $n = 10$  with 640 kOp/s and 740 kOp/s, respectively. When increasing  $n$  to 20, the throughput of Chained-Damysus decreases by a factor of  $\sim 4$ . The throughput of NxBFT drops by a factor of  $\sim 1.5$ . For  $n = 40$  compared to  $n = 20$ , throughput decreases for Chained-Damysus by a factor of  $\sim 1.8$  and for NxBFT by a factor of  $\sim 1.2$ . The figure shows the peak throughputs for the BFT client as well. MinBFT achieves the same throughput for both client variants. Chained-Damysus' and NxBFT's throughput is at least halved when using the

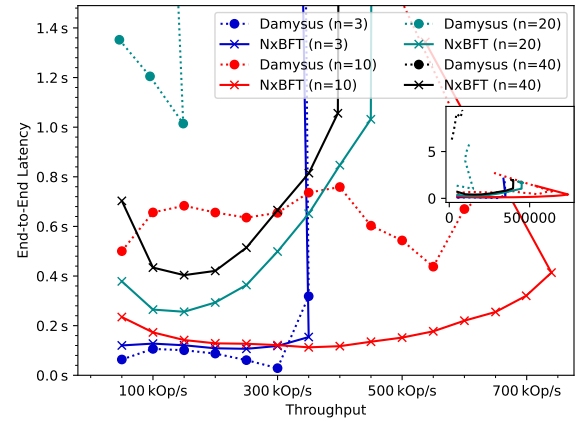


**Figure 4.** End-to-end-latency of Chained-Damysus and NxBFT for request rates between 50 kOp/s and 800 kOp/s; average of eight runs. The plot is limited on the y-axis; the full data is shown in the small window on the right.

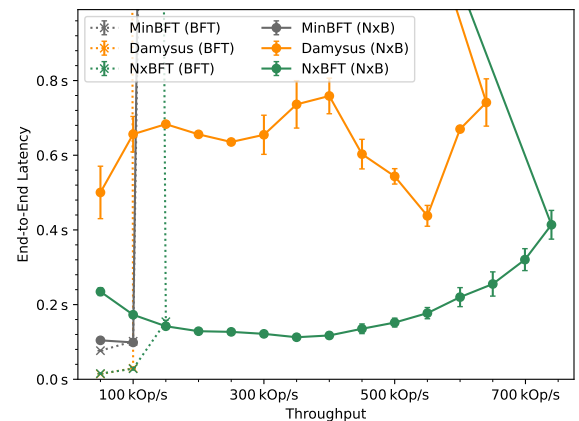


**Figure 5.** Comparison of NxB (solid) and BFT (dotted) client: end-to-end-latency of MinBFT, Chained-Damysus, and NxBFT for  $n = 10$  and request rates between 50 kOp/s and 800 kOp/s; average of eight runs. The error bars indicate the 95% confidence interval. The plot is limited on the y-axis.

BFT client. With increasing  $n$ , throughput drops up to a factor of  $\sim 8$  for NxBFT a factor of  $\sim 4.5$  for Chained-Damysus.

Figure 4 shows the corresponding latencies. To increase readability, latencies of MinBFT are omitted. Before saturating, MinBFT achieves latencies of 0.1 s for  $n < 20$  and 2.5 s for  $n \geq 20$ . For NxBFT and Chained-Damysus, the latency increases when increasing  $n$ . NxBFT achieves the best latency for  $n = 3$  and a request rate of 50 kOp/s with  $\sim 0.12$  s and stays for all configurations, before saturating, below 1 s. Chained-Damysus achieves the best latency for  $n = 3$  and a

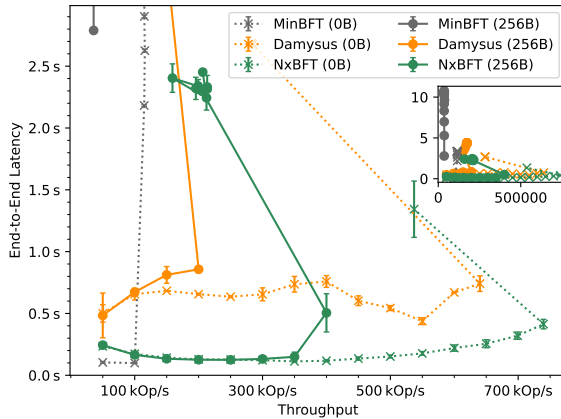


**Figure 6.** End-to-end-latency of MinBFT, Chained-Damysus, and NxBFT for  $n = 10$ , request rates between 50 kOp/s and 800 kOp/s, and payload sizes of 0 B (dotted) and 256 B (solid); average of eight runs. The error bars indicate the 95% confidence interval. The plot is limited on the y-axis; the full data is shown in the small window on the right.

request rate of 350 kOp/s with  $\sim 0.01$  s. For  $n \geq 20$ , Chained-Damysus does not achieve latencies faster than 1 s. Figure 5 compares the achieved latencies of the two client models under investigation. To increase readability, we select  $n = 10$ . Chained-Damysus and NxBFT achieve a speedup when using the BFT client (factor  $\sim 24$  for Chained-Damysus and factor  $\sim 6$  for NxBFT). MinBFT does not benefit from using the BFT client in terms of latency.

Figure 6 shows the achieved throughput and end-to-end latency of MinBFT, Chained-Damysus and NxBFT for  $n = 10$ , request rates between 50 kOp/s and 800 kOp/s (step: 50 kOp/s), and a payload of 256 B [22, 24]. We also plot the zero byte payload measures. Chained-Damysus peaks at 200 kOp/s (throughput reduced by a factor of  $\sim 3$ ) and NxBFT peaks at 400 kOp/s (throughput reduced by a factor of  $\sim 1.9$ ) while the latencies are roughly equivalent. MinBFT’s peak throughput is halved but its latency is significantly increased (factor 27).

The NxB client allows for load balancing when having a rotating leader or no leader at all. While in MinBFT the current leader has to handle *every* client connection, Chained-Damysus and NxBFT replicas handle, in expectation,  $\frac{1}{n}$ th of all client connections. Additionally, NxBFT shows the benefit of each message exchanged carrying client requests: while the workload in terms of messages exchanged and, thus, cryptographic operations performed increases when increasing  $n$ , NxBFT outperforms Chained-Damysus in terms of latency and throughput. The reduced connection load allows Chained-Damysus to scale as well, but for  $n > 10$  the increasing work to be done by the atomic broadcast eliminates those

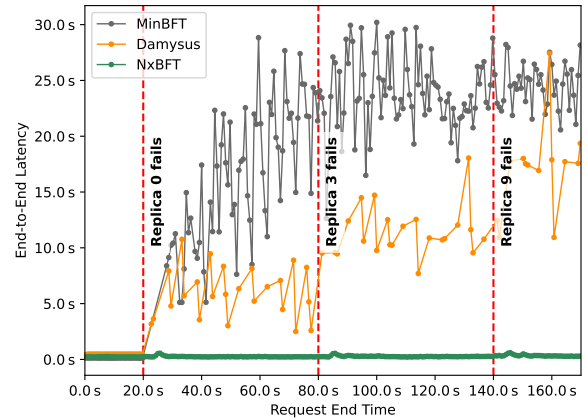


**Figure 7.** End-to-end-latency of MinBFT, Chained-Damysus, and NxBFT for  $n = 10$  and a request rate of 50 kOp/s under faults; average of ten runs. The plot shows the average end-to-end latency for requests that are successfully answered (if any) in a time buckets of size 0.75 s. After 20 s, 80 s, and 140 s, a replica fails. In case of MinBFT, replica 0 is the leader, triggering a view change.

benefits without producing as much value as it is the case for NxBFT. Our experiments also reveal a downside of the NxB client: due to the random selection of the replica, requests have to wait longer for block inclusion. Especially Chained-Damysus suffers significantly, as, in the worst case, a request has to wait  $2n$  blocks for inclusion. This is the case when the client selected the replica which just proposed a block. For MinBFT, on the other hand, the client choice does not change anything. Our experiments show that the throughput of NxBFT is primarily limited by the single thread running the atomic broadcasts’ state machine including all verification and cryptographic tasks while the overall system has an average CPU utilization of  $\sim 25\%$ . The experiments with a non-zero payload confirm this observation, as the payload mostly increases the cryptographic work (esp. hashing). A suitable parallelization in  $n$  of the cryptographic tasks may improve scaling behavior even further.

### 6.3 Performance Under Faults

We investigate the algorithms’ performance under faults for  $n = 10$  and a request rate of 50 kOp/s using the NxB client. An experiment lasts 400 s; 230 s at the start are left for warm-up. After 20 s, replica 0 crashes, after 80 s, replica 3 crashes, and after 140 s, replica 9 crashes. We selected those replicas to crash as this pattern allows Chained-Damysus to make the most progress. Figure 7 shows the average end-to-end latency of the experiment for ten repetitions.

In case of MinBFT, replica 0 is the current leader and MinBFT is forced to perform a view-change. The throughput of MinBFT stalls until the inactivity of the leader is detected (i.e.,  $5s + 3s$ ) and the view-change is performed. After the successful view-change, replica 1, the new leader is not capable to cut the backlog down, yielding increased latencies for the remainder of the experiment. The crash of replicas 3 and 9 does not increase the latency significantly. For lower request rates, MinBFT would be capable to recover fast response times within the experiment time window.

If a crashed replica does not recover, Chained-Damysus cannot recover the response times. Due to the rotating leader, each crashed replica increases the end-to-end latency clearly. Since Chained-Damysus requires a replica to be in charge for two views [23, App. B], the streamlined version of Damysus worsens this pattern. To prevent unlimited increase of Damysus’ timeouts, we do not crash four replicas. To circumvent this limitation, Damysus would require an orthogonal consensus mechanism called pacemaker [39] deciding on the current timeout value.

As all client requests are uniformly distributed across all replicas, Nx-BFT’s maximum achievable throughput degrades at most by  $\frac{c}{n}$  for  $c$  crashed replicas. For the request rate of 50 kOp/s, our experiments show that the 7 remaining replicas can handle the additional load: As soon as all clients identified a failed replica, the end-to-end latency recovers.

## 7 Discussion and Future Work

Nx-BFT’s performance achievements are built upon the assumptions regarding possible attacker behavior: The Nx-B operating model allows reducing load for clients and replicas. Load balancing in general scales with the number of replicas, however, the quadratic overhead of the broadcast layer eventually becomes the dominating factor limiting the maximum number of replicas.

The missing resilience against attacks from operators on clients can be mitigated by the application signing responses. In case of such an attack, a client can prove its correct behavior and the client state can be corrected. This procedure is a computationally less complex solution than a BFT SMR client but requires additional coordination in the case of attacks.

Operators and other third parties could attack the TEE. Such an attack would not leak any additional application data in comparison to classic BFT SMR and its mitigation requires secure multi-party computation. On the consensus layer, however, knowing coin values beforehand increases the chance for successful censorship [21], and on the broadcast layer equivocation could bring the system to a halt. We deem the probability for attacks on consensus and broadcast to be negligible in the intended deployment scenarios.

Setup and recovery require some form of synchrony to achieve liveness. We argue that, while being unconventional

for secure distributed systems research, the proposed model and assumptions are well-suited for practical deployments. Federations and consortia built upon Nx-BFT will operate a highly resilient common service. Maintenance and recovery windows can be agreed upon beforehand and peers can recover without interrupting the service. While then formally resulting in a partially synchronous system, Nx-BFT operates asynchronously once set up or recovered.

As future work, garbage collection is required: For realistic request sizes and thousands of operations per second, the required memory for storing the graph grows quickly. A garbage collection that actually deletes information, e.g., based on decided waves as in [21], however, is in conflict with asynchrony *and* the backfilling strategy described above: If a correct replica learns rather “late” (in relation to other correct replicas) that it misses some information, other correct replicas may have reached consensus and deleted this information already. The wave counter is a local variable and gives no sufficient information on the synchronization progress with other correct replicas. Scheduled maintenance time slots, as discussed above, “trivially” facilitate garbage collection: Our recovery protocol can be extended to derive a full system checkpoint, facilitating rigorous garbage collection, but, still, depending on all replicas to cooperate. From there on, implementing a voting-based reconfiguration scheme becomes easy as well.

The wave length of 4 in Nx-BFT is required to prove the convergence property of the atomic broadcast agreement property [33, Proposition 3] based on the *get core* property [34, Lemma 4]. The *get core* property is used to derive an expectation value for a correct replica being able to commit a wave. However, with a wave length of only 3 rounds, the *get core* property does not hold anymore. Overlapping waves, i.e., a round being the last round of wave  $w$  and the first round of wave  $w + 1$  as suggested by Narwhal [21], is in conflict with the *get core* property as well.

Recently, related work [3, 29, 40, 45] optimized DAG-based protocols for partial synchrony, especially the commit latency, yielding promising results. Furthermore, researchers achieved impressive performance results for asynchronous protocols in non-Byzantine environments [50]. In our opinion, these findings and the paper at hand motivate further investigation of the Nx-B operating model and of Nx-BFT-inspired approaches that combine asynchronous operation with scheduled maintenance.

## 8 Conclusion

We presented and evaluated Nx-BFT, a full-fledged TEE-based State Machine Replication approach in the “Not eXactly Byzantine” operating model. On the one hand, Nx-BFT bases its safety and liveness properties of normal case operation solely on the assumption of asynchrony and is, therefore, highly resilient. Setup and recovery, however, require some

form of synchrony. On the other hand, NxBFT shows competitive performance in terms of throughput and latency compared to the state of the art. In our opinion, further optimization and increased deployability of DAG-based approaches that use TEEs represent interesting future work.

## Acknowledgments

This work was supported by funding from the topic Engineering Secure Systems of the Helmholtz Association (HGF). We would like to thank Tilo Spannagel for his expertise during the implementation work and Oliver Stengele for his feedback on setup and recovery protocols.

## References

- [1] I. Abraham, M. K. Aguilera, and D. Malkhi. 2010. Fast Asynchronous Consensus with Optimal Resilience. In *Distributed Computing, 24th International Symposium, DISC 2010, Cambridge, MA, USA, September 13-15, 2010. Proceedings (Lecture Notes in Computer Science, Vol. 6343)*. Springer, 4–19. [https://doi.org/10.1007/978-3-642-15763-9\\_3](https://doi.org/10.1007/978-3-642-15763-9_3)
- [2] M. K. Aguilera, N. Ben-David, R. Guerraoui, A. Murat, A. Xygiak, and I. Zabolotchi. 2023. uBFT: Microsecond-Scale BFT using Disaggregated Memory. In *Proceedings of the 28th ACM International Conference on Architectural Support for Programming Languages and Operating Systems, Volume 2, ASPLOS 2023, Vancouver, BC, Canada, March 25-29, 2023*. ACM, 862–877. <https://doi.org/10.1145/3575693.3575732>
- [3] B. Arun, Z. Li, F. Suri-Payer, S. Das, and A. Spiegelman. 2024. Shoal++: High Throughput DAG BFT Can Be Fast! *CoRR* abs/2405.20488 (2024). <https://doi.org/10.48550/ARXIV.2405.20488> arXiv:2405.20488
- [4] L. Baird and A. Luykx. 2020. The Hashgraph Protocol: Efficient Asynchronous BFT for High-Throughput Distributed Ledgers. In *2020 International Conference on Omni-layer Intelligent Systems, COINS 2020, Barcelona, Spain, August 31 - September 2, 2020*. IEEE, 1–7. <https://doi.org/10.1109/COINS49042.2020.9191430>
- [5] J. Behl, T. Distler, and R. Kapitza. 2017. Hybrids on Steroids: SGX-Based High Performance BFT. In *Proceedings of the Twelfth European Conference on Computer Systems, EuroSys 2017, Belgrade, Serbia, April 23-26, 2017*. ACM, 222–237. <https://doi.org/10.1145/3064176.3064213>
- [6] N. Ben-David, B. Y. Chan, and E. Shi. 2022. Revisiting the Power of Non-Equivocation in Distributed Protocols. In *PODC '22: ACM Symposium on Principles of Distributed Computing, Salerno, Italy, July 25 - 29, 2022*. ACM, 450–459. <https://doi.org/10.1145/3519270.3538427>
- [7] M. Ben-Or. 1983. Another Advantage of Free Choice: Completely Asynchronous Agreement Protocols (Extended Abstract). In *Proceedings of the Second Annual ACM Symposium on Principles of Distributed Computing, Montreal, Quebec, Canada, August 17-19, 1983*. ACM, 27–30. <https://doi.org/10.1145/800221.806707>
- [8] A. Bessani, M. Correia, T. Distler, R. Kapitza, P. E. Verissimo, and J. Yu. 2023. Vivisecting the Dissection: On the Role of Trusted Components in BFT Protocols. *CoRR* abs/2312.05714 (2023). <https://doi.org/10.48550/ARXIV.2312.05714> arXiv:2312.05714
- [9] A. Boldyreva. 2003. Threshold Signatures, Multisignatures and Blind Signatures Based on the Gap-Diffie-Hellman-Group Signature Scheme. In *Public Key Cryptography - PKC 2003, 6th International Workshop on Theory and Practice in Public Key Cryptography, Miami, FL, USA, January 6-8, 2003, Proceedings (Lecture Notes in Computer Science, Vol. 2567)*. Springer, 31–46. [https://doi.org/10.1007/3-540-36288-6\\_3](https://doi.org/10.1007/3-540-36288-6_3)
- [10] R. Bühren, H. N. Jacob, T. Krachenfels, and J.-P. Seifert. 2021. One Glitch to Rule Them All: Fault Injection Attacks Against AMD's Secure Encrypted Virtualization. In *CCS '21: 2021 ACM SIGSAC Conference on Computer and Communications Security, Virtual Event, Republic of Korea, November 15 - 19, 2021*. ACM, 2875–2889. <https://doi.org/10.1145/3460120.3484779>
- [11] J. V. Bulck, M. Minkin, O. Weisse, D. Genkin, B. Kasikci, F. Piessens, M. Silberstein, T. F. Wenisch, Y. Yarom, and R. Strackx. 2018. Fore-shadow: Extracting the Keys to the Intel SGX Kingdom with Transient Out-of-Order Execution. In *27th USENIX Security Symposium, USENIX Security 2018, Baltimore, MD, USA, August 15-17, 2018*. USENIX Association, 991–1008. <https://www.usenix.org/conference/usenixsecurity18/presentation/bulck>
- [12] C. Cachin, R. Guerraoui, and L. E. T. Rodrigues. 2011. *Introduction to Reliable and Secure Distributed Programming (2. ed.)*. Springer. <https://doi.org/10.1007/978-3-642-15260-3>
- [13] C. Cachin, K. Kursawe, and V. Shoup. 2005. Random Oracles in Constantinople: Practical Asynchronous Byzantine Agreement Using Cryptography. *J. Cryptol.* 18, 3 (2005), 219–246. <https://doi.org/10.1007/S00145-005-0318-0>
- [14] M. Castro and B. Liskov. 2002. Practical byzantine fault tolerance and proactive recovery. *ACM Trans. Comput. Syst.* 20, 4 (2002), 398–461. <https://doi.org/10.1145/571637.571640>
- [15] B. Y. Chan and E. Shi. 2020. Streamlet: Textbook Streamlined Blockchains. In *AFT '20: 2nd ACM Conference on Advances in Financial Technologies, New York, NY, USA, October 21-23, 2020*. ACM, 1–11. <https://doi.org/10.1145/3419614.3423256>
- [16] B.-G. Chun, P. Maniatis, S. Shenker, and J. Kubiawicz. 2007. Attested append-only memory: making adversaries stick to their word. In *Proceedings of the 21st ACM Symposium on Operating Systems Principles 2007, SOSP 2007, Stevenson, Washington, USA, October 14-17, 2007*. ACM, 189–204. <https://doi.org/10.1145/1294261.1294280>
- [17] A. Clement, F. Junqueira, A. Kate, and R. Rodrigues. 2012. On the (limited) power of non-equivocation. In *ACM Symposium on Principles of Distributed Computing, PODC '12, Funchal, Madeira, Portugal, July 16-18, 2012*. ACM, 301–308. <https://doi.org/10.1145/2332432.2332490>
- [18] M. Correia, N. F. Neves, and P. Verissimo. 2004. How to Tolerate Half Less One Byzantine Nodes in Practical Distributed Systems. In *23rd International Symposium on Reliable Distributed Systems (SRDS 2004), 18-20 October 2004, Florianopolis, Brazil*. IEEE Computer Society, 174–183. <https://doi.org/10.1109/RELDIS.2004.1353018>
- [19] M. Correia, G. S. Veronese, and L. C. Lung. 2010. Asynchronous Byzantine consensus with 2f+1 processes. In *Proceedings of the 2010 ACM Symposium on Applied Computing (SAC), Sierre, Switzerland, March 22-26, 2010*. ACM, 475–480. <https://doi.org/10.1145/1774088.1774187>
- [20] V. Costan and S. Devadas. 2016. Intel SGX Explained. *IACR Cryptol. ePrint Arch.* (2016), 86. <http://eprint.iacr.org/2016/086>
- [21] G. Danezis, L. Kokoris-Kogias, A. Sonnino, and A. Spiegelman. 2022. Narwhal and Tusk: a DAG-based mempool and efficient BFT consensus. In *EuroSys '22: Seventeenth European Conference on Computer Systems, Rennes, France, April 5 - 8, 2022*. ACM, 34–50. <https://doi.org/10.1145/3492321.3519594>
- [22] J. Decouchant, D. Kozhaya, V. Rahli, and J. Yu. 2022. DAMYSUS: streamlined BFT consensus leveraging trusted components. In *EuroSys '22: Seventeenth European Conference on Computer Systems, Rennes, France, April 5 - 8, 2022*. ACM, 1–16. <https://doi.org/10.1145/3492321.3519568>
- [23] J. Decouchant, D. Kozhaya, V. Rahli, and J. Yu. 2022. *DAMYSUS: streamlined BFT consensus leveraging trusted components (Extended Version)*. Retrieved 15 Dec 2024 from <https://github.com/vrahli/damysus/blob/main/doc/damysus-extended.pdf>
- [24] J. Decouchant, D. Kozhaya, V. Rahli, and J. Yu. 2024. OneShot: View-Adapting Streamlined BFT Protocols with Trusted Execution Environments. In *IEEE International Parallel and Distributed Processing Symposium, IPDPS 2024, San Francisco, CA, USA, May 27-31, 2024*. IEEE, 1022–1033. <https://doi.org/10.1109/IPDPS57955.2024.00095>

- [25] T. Distler. 2021. Byzantine Fault-tolerant State-machine Replication from a Systems Perspective. *ACM Comput. Surv.* 54, 1 (2021), 24:1–24:38. <https://doi.org/10.1145/3436728>
- [26] C. Dwork, N. A. Lynch, and L. J. Stockmeyer. 1988. Consensus in the presence of partial synchrony. *J. ACM* 35, 2 (1988), 288–323. <https://doi.org/10.1145/42282.42283>
- [27] M. J. Fischer, N. A. Lynch, and M. Paterson. 1983. Impossibility of Distributed Consensus with One Faulty Process. In *Proceedings of the Second ACM SIGACT-SIGMOD Symposium on Principles of Database Systems, March 21-23, 1983, Colony Square Hotel, Atlanta, Georgia, USA*. ACM, 1–7. <https://doi.org/10.1145/588058.588060>
- [28] X. Fu, H. Wang, P. Shi, and X. Zhang. 2022. Teegraph: A Blockchain consensus algorithm based on TEE and DAG for data sharing in IoT. *J. Syst. Archit.* 122 (2022), 102344. <https://doi.org/10.1016/J.SYSARC.2021.102344>
- [29] N. Giridharan, F. Suri-Payer, I. Abraham, L. Alvisi, and N. Crooks. 2024. Autobahn: Seamless high speed BFT. In *Proceedings of the ACM SIGOPS 30th Symposium on Operating Systems Principles, SOSP 2024, Austin, TX, USA, November 4-6, 2024*. ACM, 1–23. <https://doi.org/10.1145/3694715.3695942>
- [30] S. Gupta, S. Rahnema, S. Pandey, N. Crooks, and M. Sadoghi. 2023. Dissecting BFT Consensus: In Trusted Components we Trust!. In *Proceedings of the Eighteenth European Conference on Computer Systems, EuroSys 2023, Rome, Italy, May 8-12, 2023*. ACM, 521–539. <https://doi.org/10.1145/3552326.3587455>
- [31] H. Howard, F. Alder, E. Ashton, A. Chamayou, S. Clebsch, M. Costa, A. Delignat-Lavaud, C. Fournet, A. Jeffery, M. Kerner, F. Kounelis, M. A. Kuppe, J. Maffre, M. Russinovich, and C. M. Wintersteiger. 2023. Confidential Consortium Framework: Secure Multiparty Applications with Confidentiality, Integrity, and High Availability. *Proc. VLDB Endow.* 17, 2 (2023), 225–240. <https://doi.org/10.14778/3626292.3626304>
- [32] Y. Jia, S. Tople, T. Moataz, D. Gong, P. Saxena, and Z. Liang. 2020. Robust P2P Primitives Using SGX Enclaves. In *23rd International Symposium on Research in Attacks, Intrusions and Defenses, RAID 2020, San Sebastian, Spain, October 14-15, 2020*. USENIX Association, 209–224. <https://www.usenix.org/conference/raid2020/presentation/jia>
- [33] I. Keidar, E. Kokoris-Kogias, O. Naor, and A. Spiegelman. 2021. All You Need is DAG. In *PODC '21: ACM Symposium on Principles of Distributed Computing, Virtual Event, Italy, July 26-30, 2021*. ACM, 165–175. <https://doi.org/10.1145/3465084.3467905>
- [34] M. Leinweber and H. Hartenstein. 2023. Brief Announcement: Let It TEE: Asynchronous Byzantine Atomic Broadcast with  $n \geq 2f+1$ . In *37th International Symposium on Distributed Computing, DISC 2023, October 10-12, 2023, L'Aquila, Italy (LIPIcs, Vol. 281)*. Schloss Dagstuhl - Leibniz-Zentrum für Informatik, 43:1–43:7. <https://doi.org/10.4230/LIPIcs.DISC.2023.43>
- [35] M. Leinweber, N. Kannengießner, H. Hartenstein, and A. Sunyaev. 2023. Leveraging Distributed Ledger Technology for Decentralized Mobility-as-a-Service Ticket Systems. In *Towards the New Normal in Mobility: Technische und betriebswirtschaftliche Aspekte*. Springer Fachmedien Wiesbaden, 547–567. [https://doi.org/10.1007/978-3-658-39438-7\\_32](https://doi.org/10.1007/978-3-658-39438-7_32)
- [36] D. Levin, J. R. Douceur, J. R. Lorch, and T. Moscibroda. 2009. TrInC: Small Trusted Hardware for Large Distributed Systems. In *Proceedings of the 6th USENIX Symposium on Networked Systems Design and Implementation, NSDI 2009, April 22-24, 2009, Boston, MA, USA*. USENIX Association, 1–14. [http://www.usenix.org/events/nsdi09/tech/full\\_papers/levin/levin.pdf](http://www.usenix.org/events/nsdi09/tech/full_papers/levin/levin.pdf)
- [37] J. Liu, W. Li, G. O. Karamé, and N. Asokan. 2019. Scalable Byzantine Consensus via Hardware-Assisted Secret Sharing. *IEEE Trans. Computers* 68, 1 (2019), 139–151. <https://doi.org/10.1109/TC.2018.2860009>
- [38] M. F. Madsen and S. Debois. 2020. On the Subject of Non-Equivocation: Defining Non-Equivocation in Synchronous Agreement Systems. In *PODC '20: ACM Symposium on Principles of Distributed Computing, Virtual Event, Italy, August 3-7, 2020*. ACM, 159–168. <https://doi.org/10.1145/3382734.3405731>
- [39] D. Malkhi and O. Naor. 2022. *The Latest View on View Synchronization*. Retrieved 15 Dec 2024 from <https://blog.chain.link/view-synchronization/>
- [40] D. Malkhi, C. Stathakopoulou, and M. Yin. 2023. BBCA-CHAIN: One-Message, Low Latency BFT Consensus on a DAG. *CoRR* abs/2310.06335 (2023). <https://doi.org/10.48550/ARXIV.2310.06335> arXiv:2310.06335
- [41] A. Miller, Y. Xia, K. Croman, E. Shi, and D. Song. 2016. The Honey Badger of BFT Protocols. In *Proceedings of the 2016 ACM SIGSAC Conference on Computer and Communications Security, Vienna, Austria, October 24-28, 2016*. ACM, 31–42. <https://doi.org/10.1145/2976749.2978399>
- [42] M. C. Pease, R. E. Shostak, and L. Lamport. 1980. Reaching Agreement in the Presence of Faults. *J. ACM* 27, 2 (1980), 228–234. <https://doi.org/10.1145/322186.322188>
- [43] M. O. Rabin. 1983. Randomized Byzantine Generals. In *24th Annual Symposium on Foundations of Computer Science, Tucson, Arizona, USA, 7-9 November 1983*. IEEE Computer Society, 403–409. <https://doi.org/10.1109/SFCS.1983.48>
- [44] F. B. Schneider. 1990. Implementing Fault-Tolerant Services Using the State Machine Approach: A Tutorial. *ACM Comput. Surv.* 22, 4 (1990), 299–319. <https://doi.org/10.1145/98163.98167>
- [45] N. Shrestha, A. Kate, and K. Nayak. 2024. Sailfish: Towards Improving Latency of DAG-based BFT. *IACR Cryptol. ePrint Arch.* (2024), 472. <https://eprint.iacr.org/2024/472>
- [46] T. Spannagel, M. Leinweber, A. Castro, and H. Hartenstein. 2023. ABCperf: Performance Evaluation of Fault Tolerant State Machine Replication Made Simple: Demo Abstract. In *Proceedings of the 24th International Middleware Conference Demos, Posters and Doctoral Symposium, Bologna, Italy, December 11-15, 2023*. ACM, 35–36. <https://doi.org/10.1145/3626564.3629101>
- [47] A. Spiegelman, B. Aurn, R. Gelashvili, and Z. Li. 2023. Shoal: Improving DAG-BFT Latency And Robustness. *CoRR* abs/2306.03058 (2023). <https://doi.org/10.48550/ARXIV.2306.03058> arXiv:2306.03058
- [48] A. Spiegelman, N. Giridharan, A. Sonnino, and L. Kokoris-Kogias. 2022. Bullshark: DAG BFT Protocols Made Practical. In *Proceedings of the 2022 ACM SIGSAC Conference on Computer and Communications Security, CCS 2022, Los Angeles, CA, USA, November 7-11, 2022*. ACM, 2705–2718. <https://doi.org/10.1145/3548606.3559361>
- [49] G. S. Veronese, M. Correia, A. N. Bessani, L. C. Lung, and P. Verissimo. 2011. Efficient Byzantine Fault-Tolerance. *IEEE Trans. Computers* 62, 1 (2011), 16–30. <https://doi.org/10.1109/TC.2011.221>
- [50] B. Wang, S. Liu, H. Dong, X. Wang, W. Xu, J. Zhang, P. Zhong, and Y. Zhang. 2024. Bundle: Asynchronous State Machine Replication Made Efficient. In *Proceedings of the Nineteenth European Conference on Computer Systems, EuroSys 2024, Athens, Greece, April 22-25, 2024*. ACM, 265–280. <https://doi.org/10.1145/3627703.3650091>
- [51] W. Wang, S. Deng, J. Niu, M. K. Reiter, and Y. Zhang. 2022. ENGRAFT: Enclave-guarded Raft on Byzantine Faulty Nodes. In *Proceedings of the 2022 ACM SIGSAC Conference on Computer and Communications Security, CCS 2022, Los Angeles, CA, USA, November 7-11, 2022*. ACM, 2841–2855. <https://doi.org/10.1145/3548606.3560639>
- [52] S. Yandamuri, I. Abraham, K. Nayak, and M. K. Reiter. 2022. Communication-Efficient BFT Using Small Trusted Hardware to Tolerate Minority Corruption. In *26th International Conference on Principles of Distributed Systems, OPODIS 2022, December 13-15, 2022, Brussels, Belgium (LIPIcs, Vol. 253)*. Schloss Dagstuhl - Leibniz-Zentrum für Informatik, 24:1–24:23. <https://doi.org/10.4230/LIPIcs.OPODIS.2022.24>
- [53] M. Yin, D. Malkhi, M. K. Reiter, G. Golan-Gueta, and I. Abraham. 2019. HotStuff: BFT Consensus with Linearity and Responsiveness. In *Proceedings of the 2019 ACM Symposium on Principles of Distributed Computing, PODC 2019, Toronto, ON, Canada, July 29 - August 2, 2019*. ACM, 347–356. <https://doi.org/10.1145/3293611.3331591>